Available online at www.sciencedirect.com
ScienceDirect
Nuclear Instruments and Methods in Physics Research A 591 (2008) 353–366
NUCLEAR INSTRUMENTS & METHODS IN PHYSICS RESEARCH Section A
www.elsevier.com/locate/nima

Extension of the operational lifetime of the proportional chambers in the HERMES spectrometer

S. Belostotski[a], S. Frullani[b], G. Gavrilov[a,*], O. Miklukho[a], L. Shchipunov[a], D. Veretennikov[a], V. Vikhrov[a]

[a]Petersburg Nuclear Physics Institute, Russian Academy of Science, Gatchina, St. Petersburg district 188350, Russia
[b]Physics Laboratory, Istituto Superiore di Sanitá and INFN Sezione di Roma-gruppo Sanitá, viale Regina Elena 299, Rome I-00161, Italy

Received 1 October 2007; received in revised form 1 February 2008; accepted 2 March 2008
Available online 14 March 2008

Abstract

The experience of the extension of the proportional chambers lifetime at the HERMES (DESY) experiment is presented. A non-invasive technique against the aging process while continuously operating the detectors in the gap of the HERMES spectrometer magnet was performed. It was found that adding 0.14% water to the $65\%Ar + 30\%CO_2 + 5\%CF_4$ gas mixture perfectly cancelled the appearance of self-sustained current (Malter effect). The studies of the remedy for the lifetime extension were performed with the test prototypes of the original proportional chambers. For the complete recovery of the aged test proportional chambers a special training method was developed as well. Training of the aged proportional chamber at $80\%CF_4 + 20\%CO_2$ mixture glow discharge with reversed high voltage demonstrated a complete recovery of the detector.

PACS: 29.40Cs; 29.40Gs; 55.77Bn

Keywords: Fast aging; Intensive irradiation; Aging curing; Malter current

1. Introduction

In the HERMES spectrometer [1,2] the momentum of charged particles is derived by tracking devices (multiwire drift chambers) located upstream and downstream of a dipole magnet, and external to the high field region.

The proportional chambers installed inside the spectrometer dipole magnet together with the front part of the HERMES tracking system are capable of reconstructing the momenta of particles without using position information from the drift chambers located downstream of the magnet. This allows the analysis of low momentum particles strongly bent by the magnetic field. These proportional chambers will be called magnet chambers (MCs) throughout the text. The magnet proportional chambers were installed in the HERMES spectrometer dipole magnet in the fall of 1994.

*Corresponding author. Tel.: +7 813 71 460 42; fax: +7 813 71 379 76.
E-mail address: gavrilov@mail.desy.de (G. Gavrilov).

0168-9002/$ - see front matter © 2008 Elsevier B.V. All rights reserved.
doi:10.1016/j.nima.2008.03.009

2. Aging of the proportional chambers in HERMES

2.1. Design of the proportional chambers

The magnet proportional chambers are mechanically assembled in two blocks (top and bottom) installed in the spectrometer magnet above and below the septum plate, see Fig. 1.

Each MC block consists of three modules MC1, MC2, MC3. A MC module contains three anode planes of sense wires U, X and V interleaved with the cathode wire planes. The sense wires with 2 mm spacing are made of 25 μm diameter gold-plated tungsten. The U and V wires are tilted at $\pm 30^\circ$ with respect to the vertical X wires. Cathode planes are made of 90 μm diameter bronze (not gold plated) wire with 0.5 mm spacing. The distance between anode and cathode planes is 4 mm. The working gas mixture is Ar (65%), CO_2 (30%) and CF_4 (5%). A detailed description of the MC design is given in Ref. [1].

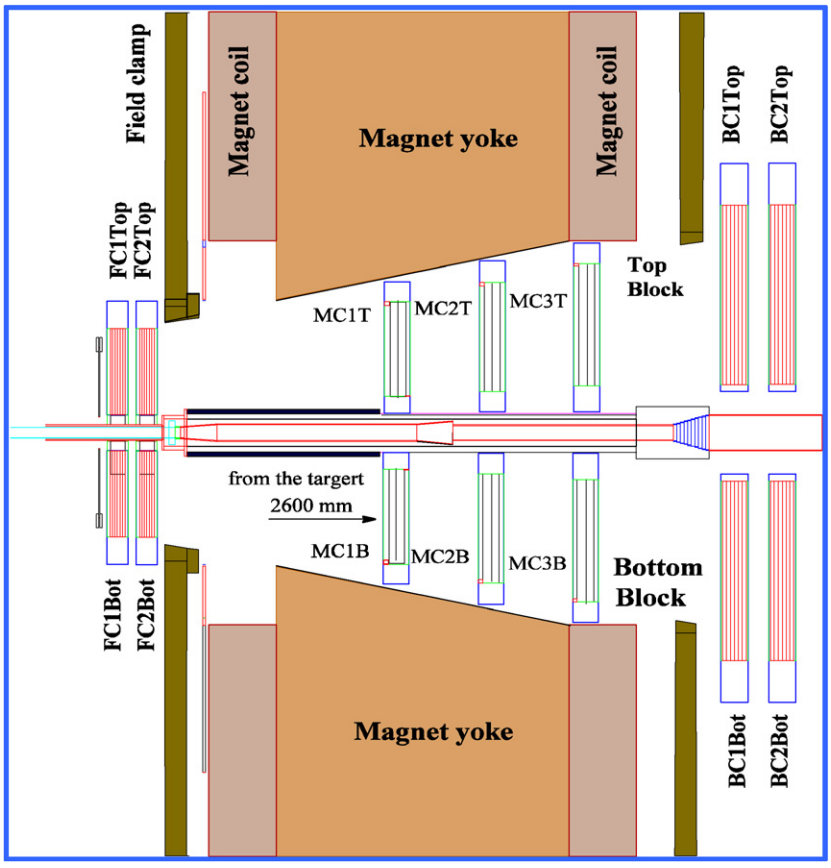

Fig. 1. Side view of the MC set up inside the dipole magnet. FC and BC indicates the forward (FC) and back (BC) drift chambers, which are located upstream and downstream of a dipole magnet, respectively.

2.2. Aging effect in the MCs

An estimate of the integrated charge accumulated by the MCs during 8 years of operation at HERA is given in Table 1. The integrated charge is presented in units of charge per cm of anode wire length. According to our evaluation the MCs currents shown also in Table 1 cannot be related to the charged particles load. The currents are consistent with that expected from the synchrotron light accompanying the electron (positron) beam of the HERA collider (the dark current in the MCs is negligible). As one can see from Table 1 the synchrotron irradiation in the HERMES spectrometer area has a large up/down asymmetry. The aging problem is significant only for the top block modules.

Since HERMES commissioning in 1995, the MCs were inspected and disassembled for repair several times, which included high voltage training and cleaning with alcohol of both cathode and anode planes. The onset of aging was noticed in the inspection in the year 2000. During a high voltage test of the MC1 and MC2 top chambers with a ^{90}Sr β-source, a sharp rise of the current not associated with ionisation was observed. Removal of the radioactive source and even lowering the high voltage by 200 V did not suppress the self-sustained current. Inside of the disassembled MC1 top chamber dark spots were found on the wires of the cathode plane. This fact together with the self-sustained current ignited by the ^{90}Sr β-source is evidence for the so-called ''Malter effect'' [3,4].

Table 1
Accumulated charge over 8 HERMES years

Modules	Top block		Bottom block	
	Average current (μA)	Charge (C/cm)	Average current (μA)	Charge (C/cm)
MC1	1.5	7.0×10^{-3}	0.2	0.2×10^{-3}
MC2	1.0	3.5×10^{-3}	0.15	0.15×10^{-3}
MC3	0.7	2.0×10^{-3}	0.1	0.1×10^{-3}

This effect is caused by appearance of an insulating layer of deposits or oxide on the cathode. An electric dipole is formed across this insulating layer at the cathode due to positive ions produced by avalanche at the anode wire. Together with an induced image charge on the cathode, a positive charge collects on the surface and a large electric dipole field is produced. The result is that the threshold for secondary electron emission is exceeded, and electrons are ''pulled'' from the cathode wires by the electric field. Many of the emitted electrons penetrate the insulating layer, enter the gas and drift to the anode. The resulting avalanches enhance the strength of the dipole field and the field

emission of electrons. This positive feedback results in a large current, which can only be stopped by turning off the high voltage. Another outcome of the charged insulated layer on the cathode wires is a partial screening of the electric field in the proportional chamber that results in a moderate drop of the efficiency.

Neither cleaning of the deteriorated chambers with glow discharge in N_2 and in the working gas mixture, nor cleaning of the cathode planes with alcohol, helped to alleviate the problem. Fig. 2 shows the dependence of the beam ionisation current on the high voltage for the top chambers. As one can see in Fig. 2, both MC1 and MC2 top block chambers demonstrated a sustained current, which appeared at the top chambers in the MC1 U-plane and MC2 V-plane at HV = 2925 and 3000 V, respectively. In case of high background conditions the sustained current started even about 100 V lower.

Another devastating consequence of the aging process is a drop of the proportional chambers efficiency. This effect is most likely due to polymerisation on the anode wires and may be the cause of reduction in signal amplitude. Fig. 3 shows the MC efficiency measured with the HERA beam in 2003 (△) and 2004 (▼) for the Top Block. A progressively greater reduction of the MC1, MC2 top chambers efficiency is seen. Efficiency dependence is shorted because of the Malter current at HV = 2900 V for U-plane MC1 top and at HV = 2975 V for V-plane MC2 top chambers.

To summarise, in 2004, the MC1 and MC2 top block chambers were in dangerous situation. It seemed probable that due to both the Malter effect and the anode aging the damaged chambers would soon fail. An early attempt to improve the MC performance by training with standard gas mixture of the aged planes under inversed high voltage resulted in breaking of an anode wire of the MC2 top

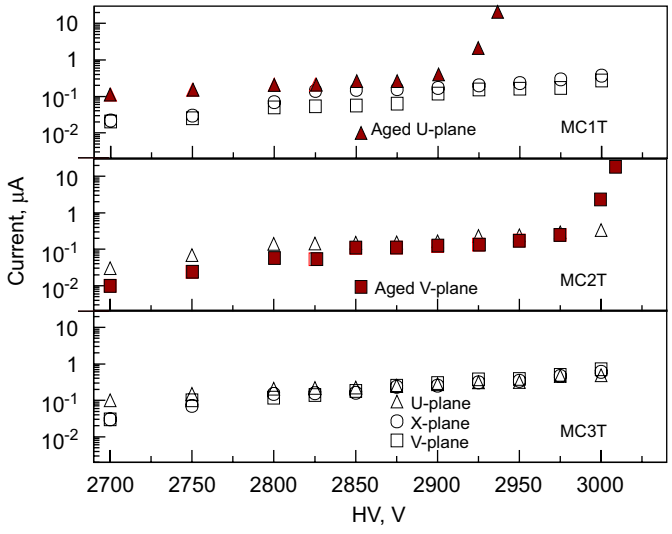

Fig. 2. Dependence of the beam ionisation current from the high voltage for the top chambers. Sustained current appears in the MC1 U-plane and MC2 V-plane top block chambers at HV = 2925 and 3000 V correspondingly.

X-plane. Because of the impossibility to access this plane, it is turned off since 2003.

3. Choice of the recovery method for the MCs

3.1. Possible remedies against MC degradation

A way to reduce the Malter effect is to use gas additives both to suppress polymerisation and to increase the conductivity of the insulating layer [3,5,6]. These additives usually are vapours of water or alcohol.

Water vapour (500–2000 ppm) prevents the start of polymerisation. Molecules of water exchange charge with some avalanche ions that would otherwise have polymerised on the cathode. Water never polymerises by itself. Therefore, the addition of water reduces the polymerisation rates. If the water is introduced after the deposits have formed, it tends to stabilise detector operation and prevents the Malter effect.

Water also makes all surfaces in the detector slightly more conductive, thus preventing the accumulation of ions on the polymer layer responsible for the gain degradation and increase of sustained current, see Ref. [5]. The inevitable increase in conductivity on frames and spacers is not always acceptable and needs a further preliminary study. Good examples of detectors where water restored detector efficiency are the drift chambers of SLD [6], BarBar [7] and ZEUS [8].

Alcohol molecules have large dipole moments, and they may, therefore, be attached directly to the electrodes. Alcohol molecules perform charge exchange more readily than water. Once the deposits have formed, the introduction of alcohol (1–2%) tends to stabilise the operation and to prevent the Malter effect. Alcohol molecules absorb UV photons originated from ion–electron recombination on the cathode or in avalanche. In principle, various alcohol dissociation products, such as CH_2O_2, C_2H_4O or $C_2H_4O_2$, can react with aluminium frames of the MCs and create highly resistant oxides. However, the main danger of the alcohol additives in the gas mixture is a solvent action that can cause the detector components swelling and expansion of plastic materials [5]. For example, materials that can be affected are the entrance window of the MC, made of aluminised Mylar and the electrode frame, made of STEF fibreglass, a G-10 analogue.

3.2. Test setup and method of study

The MCs are located in the spectrometer magnet gap and are not accessible for testing. Thus, to optimise the amount of water providing the stabilisation of the MC, investigation on the test chambers have been performed. This is a typical approach of many experiments [7,8], because, usually, the working conditions are unique and dependent on the design peculiarities of each detector.

For the aging test four test proportional chambers were produced similar to the MC design. Two of these

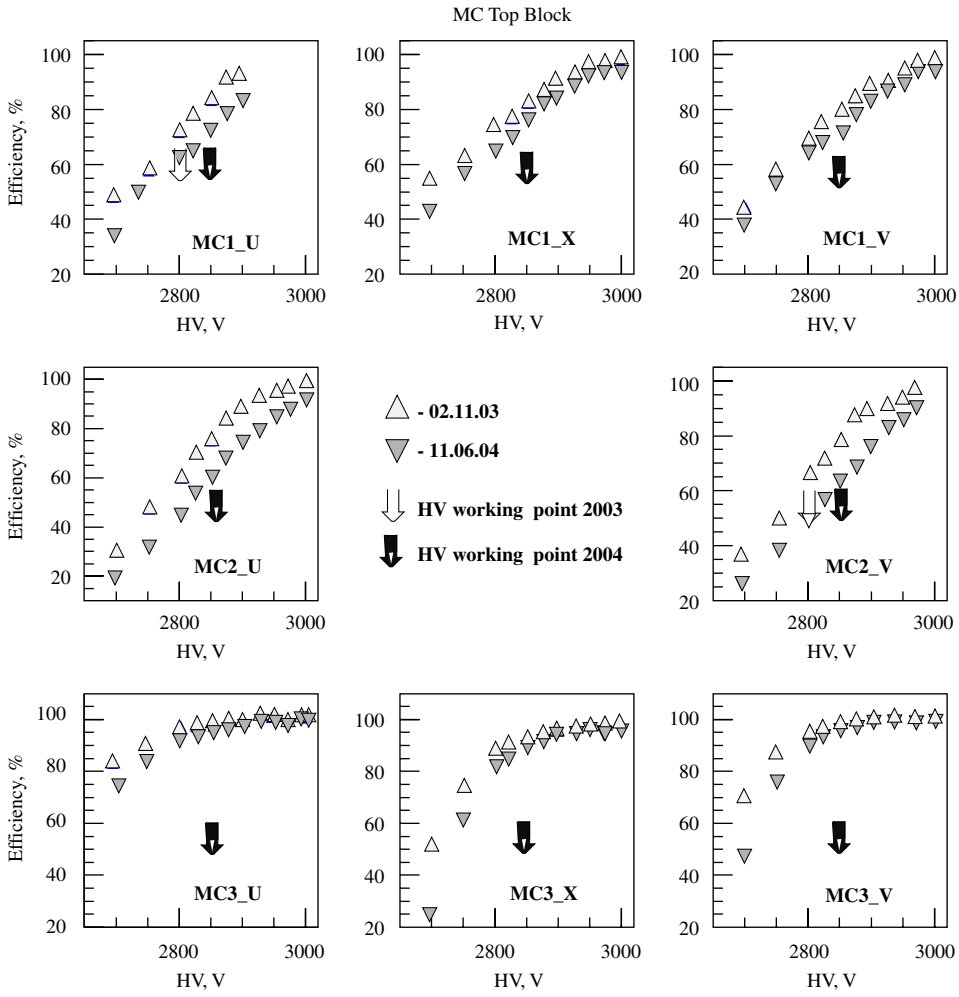

Fig. 3. Magnet chambers efficiency for the top block chamber versus high voltage at standard threshold used for data taking measured in the HERA positron beam in 2003 (△) and 2004 (▼).

prototypes had anode wire 15 μm in diameter to make them more sensitive to the anode aging than MCs with 25 μm wire in diameter. Cathode planes of the prototypes consisted of 90 μm diameter bronze wires, which were oriented perpendicular to the anode wires. The active area of the test chamber was $11 \times 11\,\mathrm{cm}^2$.

An intense ^{90}Sr β-source with an integrated intensity of $I = 10\,\mathrm{MHz}$ (in 4π) was used to irradiate the test chamber. An irradiation zone of $S^{\mathrm{spot}} = 5\,\mathrm{cm}^2$ was defined by 7 mm diameter collimator. The size of the irradiation zone was confirmed both by GEANT simulation of the irradiation geometry and by exposing a photographic film positioned in the place of the entrance window. The measurements of the detector properties usually were performed after 5–6 h of exposure. When the ^{90}Sr source was removed, the dark current and count rates (with and without ^{55}Fe γ-rays source) were measured both from irradiated and from wires that were not radiated. The gas gain at these zones was monitored by measurement of the escape peak position of the ^{55}Fe γ-ray spectrum as in Refs. [3,9]. Resulting gas gain was scaled to non-irradiated undamaged areas of the anode wires. The same preamplifier was used for all measurements to avoid calibration errors. To stimulate the appearance of the Malter current in the aged chamber, the whole active area after each irradiation run was scanned as well, by a $I = 1\,\mathrm{MHz}$ ^{90}Sr β-source with a 2 mm diameter collimator. The high voltage during this test was 200 V above the working point (W.P.).

To provide similar aging conditions for the aging study, we measured the gas gain for both types of test chambers. The gain was determined as a ratio of the ^{90}Sr β-source ionisation current in the gas gain mode to the current of the ionisation plateau. Then we chose the W.P. of the high voltage such that all of the test chambers had a gas gain $G = 5.5 \times 10^4$ similar to that of the MCs in the HERMES experiment. As one can see in Fig. 4, the W.P. for the TC1 test chamber with 15 μm anode wire is 2750 V and for the TC3 test chamber with 25 μm anode wire it is 2850 V.

During the aging test cathode aging manifests itself by spreading the deposits produced in the localised irradiation zone along the whole cathode plane area that is $S^{\mathrm{total}} = 100\,\mathrm{cm}^2$ for the test chamber. Anode deposits are concentrated in a much smaller region and anode ageing proceeds much faster. We suppose that to obtain the

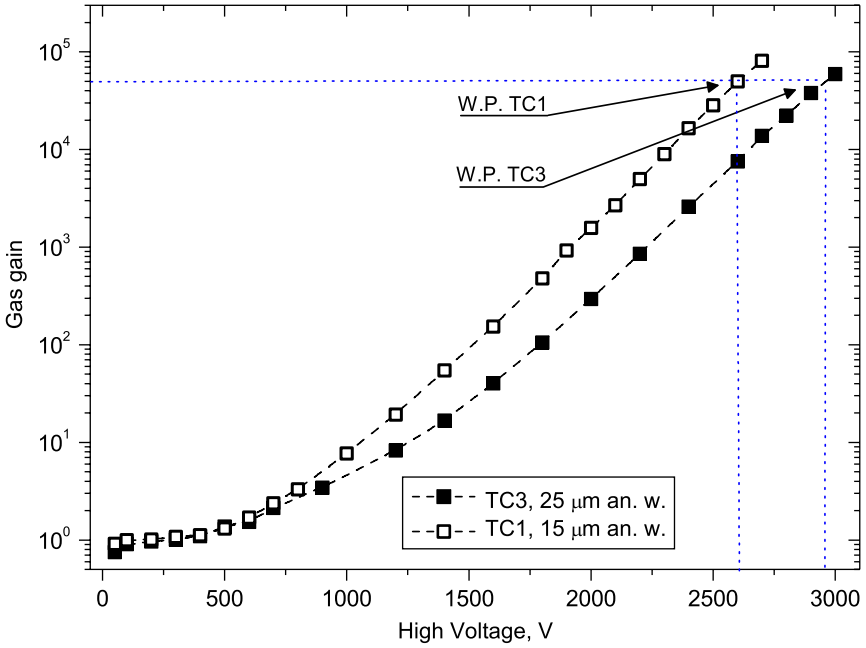

Fig. 4. Gas gain dependence on the high voltage for the test chambers TC1 with anode wire diameter 15 μm and TC3 with anode wire diameter 25 μm.

equivalent charge for the cathode aging, the collected charge in the irradiation zone S^{spot} should be distributed over the entire cathode surface, see Ref. [9].

Then since the maximum charge obtained by the MCs at the HERMES irradiation conditions is $Q_{wire}^{HERMES} = 10\,mC/cm$, the charge to be accumulated during the test by the anode wires, which provides $Q_{cathode}^{test} = Q_{wire}^{HERMES}$, was evaluated as

$$Q_{anode}^{test} = Q_{cathode}^{test} \times S^{total}/S^{spot} \approx 200\,mC/cm. \quad (1)$$

Having the gas gain similar in the test chamber to that of MCs, i.e. $G = 5.5 \times 10^4$, a rate of the charge accumulation per day may be evaluated as

$$Q_{anode}^{day} = I \times G \times N_{track} \times T_{sec} \approx 30\,mC/cm \quad (2)$$

where $N_{track} \approx 90$ number of ionisation electrons per track in the test chamber, $I = 400\,kHz/cm$ is the intensity of ^{90}Sr β-source per wire, $T_{sec} = 86400\,s/day$. Thus the time necessary to cause a similar cathode aging effect in the test chamber from Eqs. (1) and (2) was determined to be about a week of irradiation.

The value of $Q_{anode}^{test} = 200\,mC/cm$ in the irradiated zone is much higher than that in the MCs. Due to anode aging, we expected a decrease in the gas gain G and then a decrease in the ionisation current. In order to obtain a desired cathode aging, the test proportional chambers were irradiated in three test points. This allowed us to have a stable charge accumulation rate. It must be noted as well that in our evaluations a uniform distribution of the cathode deposits was assumed. A gas flow rate of 7 ml/min in the test chambers provided the same chamber-volume refreshing rate of 33 Vol/day as in the HERMES chambers. A branch line from the MCs gas system provided the gas supply.

3.3. Aging of the test proportional chambers

3.3.1. Aging of the anode wires

The aging test of the prototype test chambers reproduced the observed signs of aging in the experiment. To measure the test chamber degradation the relative gas gain was measured as a ratio of the ^{55}Fe amplitudes (escape peak position) in the irradiated and reference undamaged points. Fig. 5 shows the relative gas gain drop of 22% at accumulated charge of about $Q_{anode}^{test} = 10\,mC/cm$ during the test with a standard MCs gas mixture. This properly explains the inefficiency of the MCs presented in Fig. 3.

Adding 0.14% H_2O to the standard 65%Ar + 30% CO_2 + 5%CF_4 gas mixture led to a stable gas gain until an accumulated charge of 30 mC/cm. As one can see, both types of test chambers demonstrated stability until a dose equivalent to almost 30 years of HERMES operation. Water did not cure, however, already damaged parts of the anode wires. Despite the high accumulated charge, amplitude degradation was observed only in the irradiated zones of the test chamber. To illustrate the progression of anode aging the ^{55}Fe response was recorded with a 4 mm step along the anode wires. Fig. 6 shows a front view of the test chamber with the ^{90}Sr irradiation-zones and nine test points for the ^{55}Fe γ-source monitoring.

One can also see the results of two amplitude scans with an ^{55}Fe γ-source. The signal is plotted against the test point location without irradiation at test points 1, 4, 7 and with irradiation at test point 5. A strong reduction of the amplitude is seen. The accumulated charge at the test-point 5 is $Q_{anode}^{point\ 5} = 32\,mC/cm$. The aging affected only the exposed parts of the anode wires that passed through the irradiated zone at the test points 2, 5, 8, but did not affect the test points outside of the irradiated area. The total

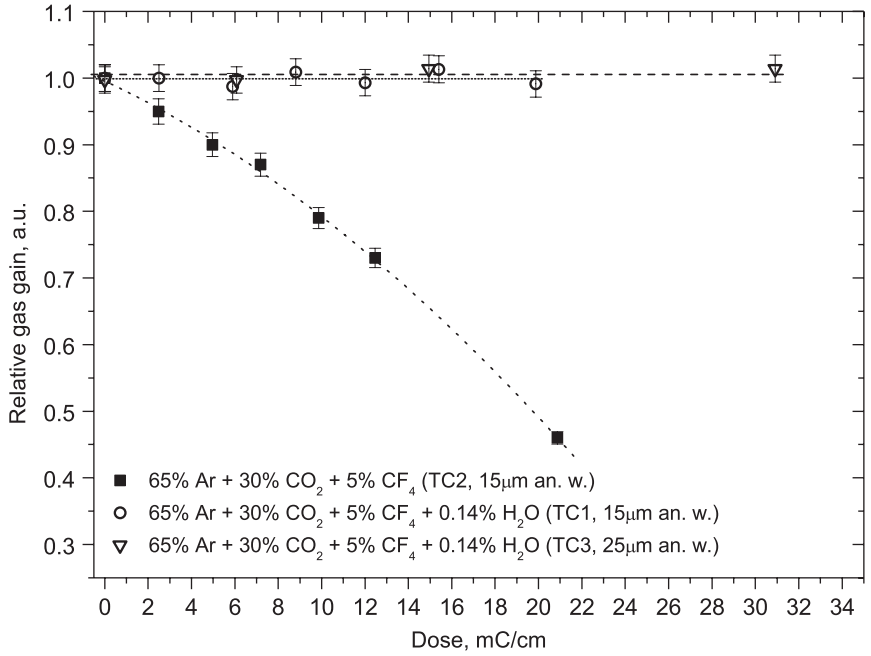

Fig. 5. Dependence of the relative gain in the irradiated zone versus accumulated charge by the anode wires. Black squares correspond to the test with standard MCs gas mixture. White cycles and triangles correspond to the test of both types of proportional chambers with addition of 0.14% H_2O to the standard gas mixture.

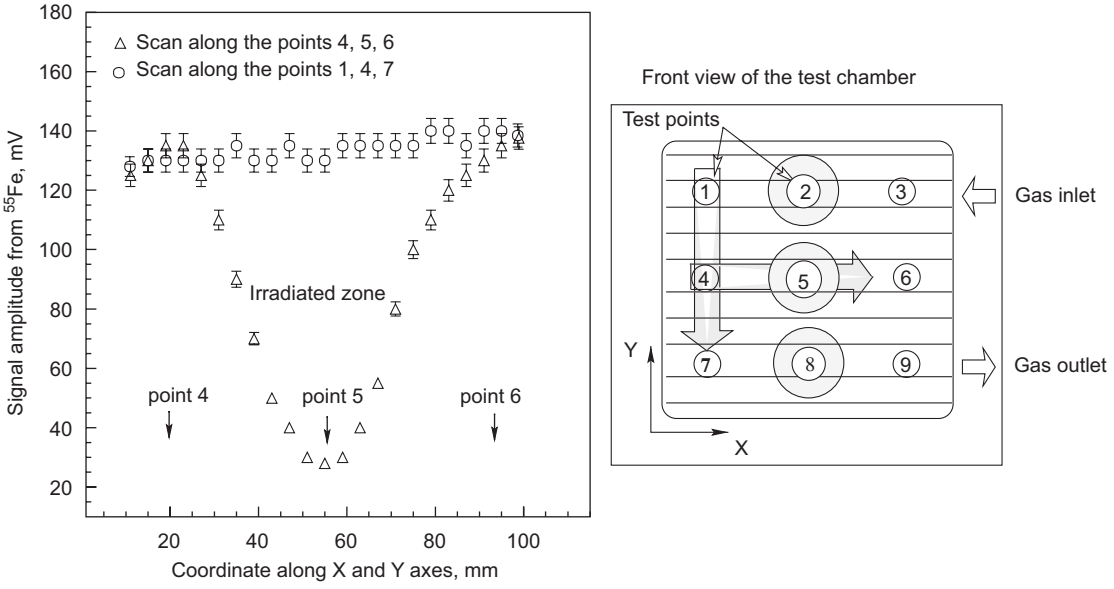

Fig. 6. The amplitude scans with an ^{55}Fe γ-source along the *Y*-axis through non-irradiates points 1,4,7 and along the *X*-axis through one of the irradiated zones in the point 5. The anode wires are shown in a front view of the test chamber by the lines directed along the *X*-axis. The accumulated charge in the irradiated zone at point 5 is equal to $Q_{\text{anode}}^{\text{point 5}} = 32\,\text{mC/cm}$.

charge accumulated by the test proportional chamber anode wires was

$$Q_{\text{anode}}^{\text{test}} = Q_{\text{anode}}^{\text{point 2}} + Q_{\text{anode}}^{\text{point 5}} + Q_{\text{anode}}^{\text{point 8}} = 28 + 32 + 35 = 95\,\text{mC/cm}.$$

The amplitudes observed by scanning along the non-irradiated test-points 1, 4, 7 varies only by 10%. This variation is within the range of the detector's design accuracy.

3.3.2. Aging of the cathode wires

Cathode aging appeared at accumulated charge according to Eq. (1) of $Q_{\text{cathode}} = 4.75\,\text{mC/cm}$. Fig. 7 shows two ^{90}Sr scan profiles, along the anode wires one through the 4, 5, 6 and through the 7, 8, 9 test-points. One notes the appearance of a self-sustained current of 15–20 μA at the non-irradiated area marked as "Malter zone". During monitoring, the collimated ^{90}Sr source merely ignited the self-sustained current at this area and only removing the

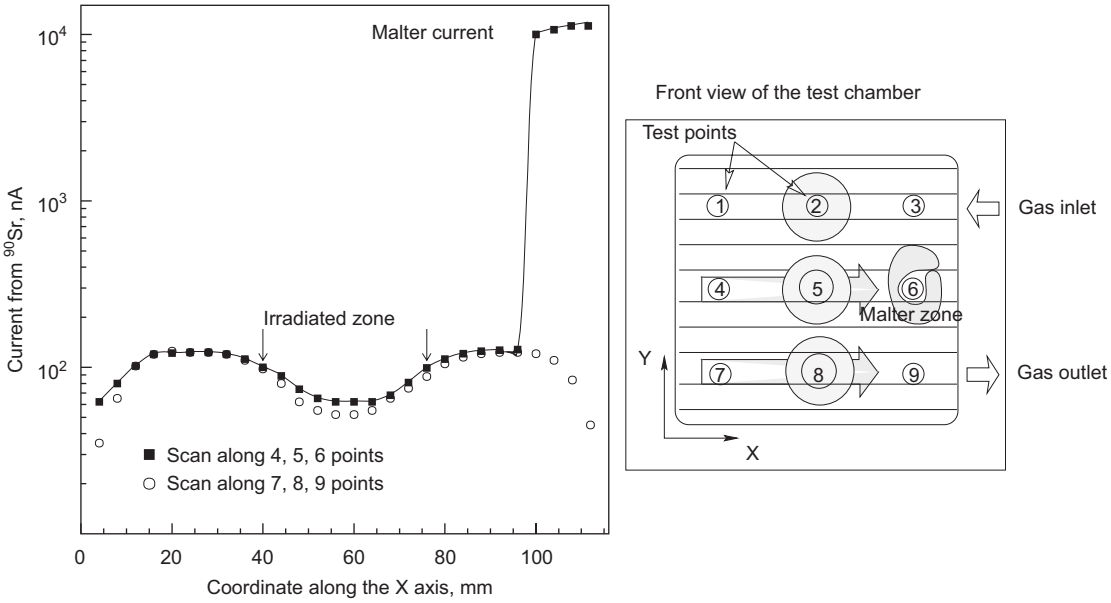

Fig. 7. Scans by the collimated ^{90}Sr β-source along the anode wires. The total accumulated charge in the irradiated zones 2, 5 and 8 is $Q^{test}_{anode} = 95\,mC/cm$ that corresponds to $Q_{cathode} = 4.75\,mC/cm$ for the cathode wires. An area where the ^{90}Sr ignited the self-sustained current is marked as 'Malter zone'.

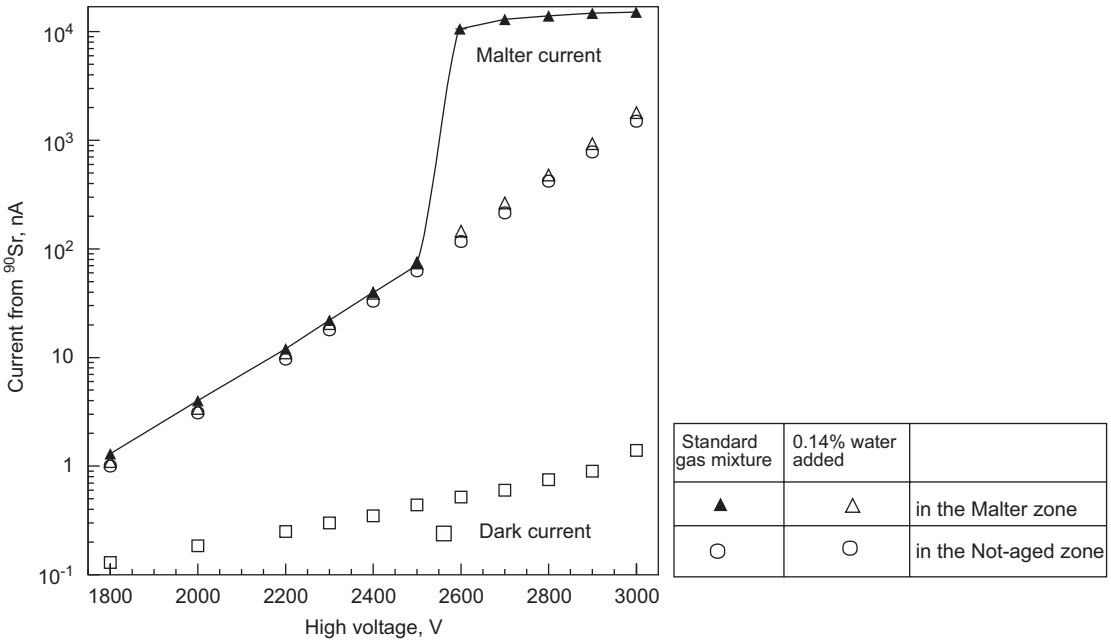

Fig. 8. Dependence of the ^{90}Sr ionisation current and dark current from high voltage.

high voltage stopped this current. This is a typical manifestation of the Malter effect. The other parts of the cathode behave as usual and demonstrated only ionisation current from ^{90}Sr. Early manifestation of the Malter effect in the test proportional chambers compared with MCs can be explained by the higher 1 MHz intensity of the monitoring ^{90}Sr in comparison with $0.0005\,MHz/cm^2$ intensity in the experiment. Also note ventilation between the inlet and outlet points in the test chamber may have been insufficient. A study of the damaged zone has shown that it was relatively small in size, about $2 \times 4\,cm^2$. This observation is consistent with descriptions of the Malter effect that were given by others authors [3,6].

Fig. 8 presents the ^{90}Sr ionisation current versus the high voltage measured at the area touched by the Malter effect (▲,△) and unexposed in the reference test-point 3 (○) (see Fig. 7). Two sets of measurements were taken. The first data collection was performed with MCs standard gas mixture (▲) and the second measurement with addition to the gas mixture of 0.14% H_2O (△). During both sessions the values of the measured current in the unexposed test-point had very small variation (○). The addition of 0.14%

H_2O to the working gas mixture practically eliminated the Malter effect. Subsequent monitoring with ^{90}Sr of the sensitive area whole test chambers did not show any sign of self-sustained current. Returning to a dry gas mixture very soon caused the repeated appearance of the self-sustained current in the sixth test-point area. The measurements of the dark current (□) do not show any noticeable change both in case of the dry and wetted gas mixtures.

3.3.3. Study of the reason of fast aging

The charges provoking both anode and cathode aging in the MCs are not typical for $65\%Ar + 30\%CO_2 + 5\%CF_4$ as working gas mixture. Therefore, as a most probable specific reason for aging we supposed oil pollution from the pipes in the gas supply system. To prove that the contaminants came from the gas supply system an aging test run with test prototype TC2 was performed using gas supplied from a pre-mixed bottle. The purity of the gas components was Ar—99.996%, CO_2—99.995 and CF_4—99.995%. During the test the prototype chamber accumulated up to 250 mC/cm and exhibit a stable operation without any signs of aging.

3.4. Hydration of the working gas mixture

Thus the addition of a small amount of water to the gas mixture alleviated the aging problem in the test proportional chambers. This solution also extended the lifetime of the HERMES MCs. Although the addition of water cannot reverse the aging process, it stops further degradation and prevents the appearance of the Malter current. The latest allows increasing the high voltage in the damaged MC modules by as much as 50–100 V.

Fig. 9 shows the scheme of the hydration system for the MCs. The HERMES proportional MCs have an open gas supply system, which is dependent upon atmospheric pressure, and varies by ± 20 mbar.

The gas mixture pressure in the detector and gas system is about $P_{syst} = 1050$ mbar. The composition of the gas mixture is maintained by the Multi Gas Controller MKS 647B (**1**), which operates three mass flow-controllers. Here the flow-controllers (**2**, **3**, **4**) provide standard gas mixture in proportion of 65%Ar, 30%CO_2 and 5%CF_4. Each flow-controller has a working range up to 1000 sccm. All gas mixture components are premixed in a dedicated 5 l volume (**5**). Then the gas flow divides into two parts in a 9:1 ratio. One part of the gas flow is led through a Vapour Source Controller (VSC, **6**) which is used to control an amount of water vapour. The VSC is based on a bubbler filled with water and a Peltier Chilling Incubator [10]. The temperature inside the incubator is stabilised in the range from 4 to 70 °C with an accuracy of ± 0.3 °C. After passing through the bubbler the gas mixture in the pipe coil inside of the incubator reaches the Dew point temperature T, which defines the water vapour content. The water vapour concentration may be evaluated as

$$C_{water} = \frac{p_{vapour}(T)}{P_{syst}} \times 100\% \quad (3)$$

where $P_{vapour}(T)$—saturation vapour pressure and $P_{syst} = 1050$ mbar—pressure in the gas system. Having been establish in the Peltier Chilling Incubator at $T = 12$ °C the water vapour pressure is set to $p_{vapour}(T) = 15$ mbar. Hence, on output of the VSC, the gas mixture contains 1.4% of water. Mixing of one part of the hydrated and nine parts of the dry flows results in 0.14% of water in the working gas mixture. For monitoring the moisture content a Dew point chilled mirror hygrometer (MBW CH-5430) is used.

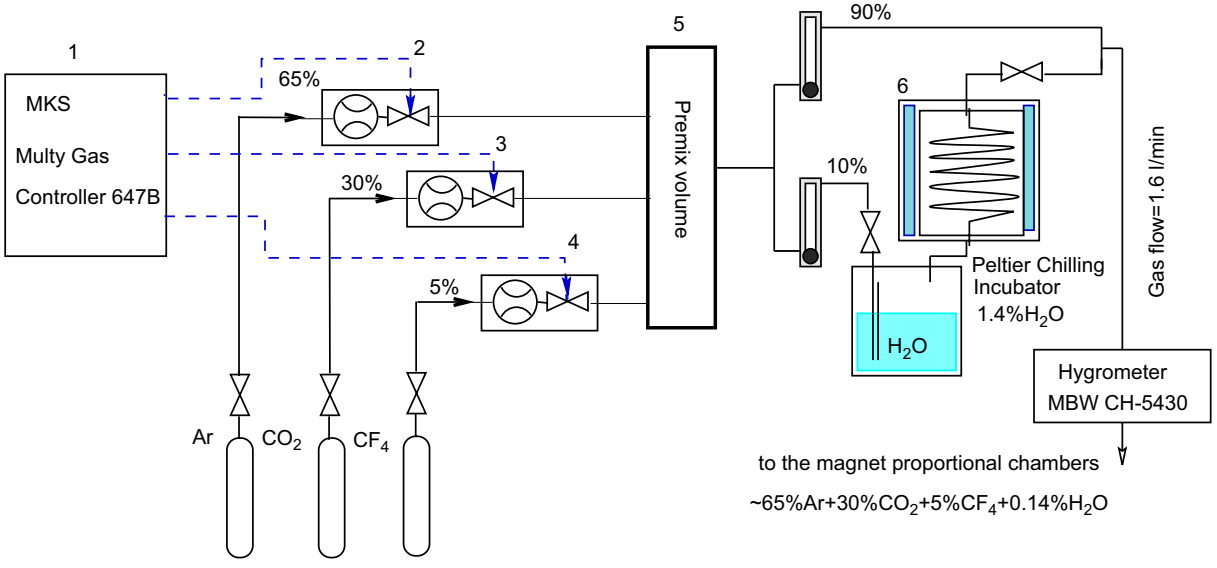

Fig. 9. Scheme of the magnet proportional chambers hydration system.

4. Recovery of the MCs in the experiment

The hydration of the MC gas mixture started at the beginning of 2005. After 24 h of flow with the wetted gas mixture, the MCs high voltage scan in the electron beam demonstrated the absence of any self-sustained current in the modules up to the W.P. of 3000 V. This improvement was stable in time. In Fig. 10, the dependence of efficiency on the high voltage is shown measured with a dry gas mixture (▲) in 2004 and with a hydrated gas mixture (△) measured after 2 months of application in 2005. As one can see, the scan is no longer shortened by the Malter current for MC1 U-plane or MC2 V-plane top-block chambers. Therefore, to compensate for the degraded efficiency, the high voltage W.Ps. (⇓) in the MC1 and MC2 top chambers were increased by 50–100 V as shown in Fig. 10. This improved the efficiency of the aged planes at 20–25%. The presence of the anode deposits limited high voltage increase because of the sparking risk.

During the high voltage scan, the MC planes demonstrated higher efficiency than before. For example, the MC1 U-plane at a W.P. of HV = 2850 V improved in efficiency from 76% to 85%. This can be explained by water preventing the accumulation of positive ions on the cathode wires and thus screening the electrical field. It might be supposed as well that in electron avalanche, predominantly CF_3^+ and F^- are produced near the anode wire [11]. Thus having a hydrated gas mixture, atomic fluorine reacts with water forming the stable HF molecule: $H_2O + F \rightarrow HF + OH$. This molecule is not very reactive, but together with water forms hydrofluoric acid, which could partially etch the siliceous deposits on the anode wire. Usually this kind of etching is dangerous for gaseous detectors [3,5,6,11], but for MCs at rather small irradiation current 1.5 μA per 0.4 m^2 and at a low water content 0.14% it can play a positive role.

5. Curing of the aged test proportional chambers

As seen from the previous discussion, the aging seriously affected only two chambers of the top block. Addition of water vapour in the gas mixture limited the aging phenomenon both in the deteriorated and safe MCs. Later we wanted to study the possibility of curing the aged

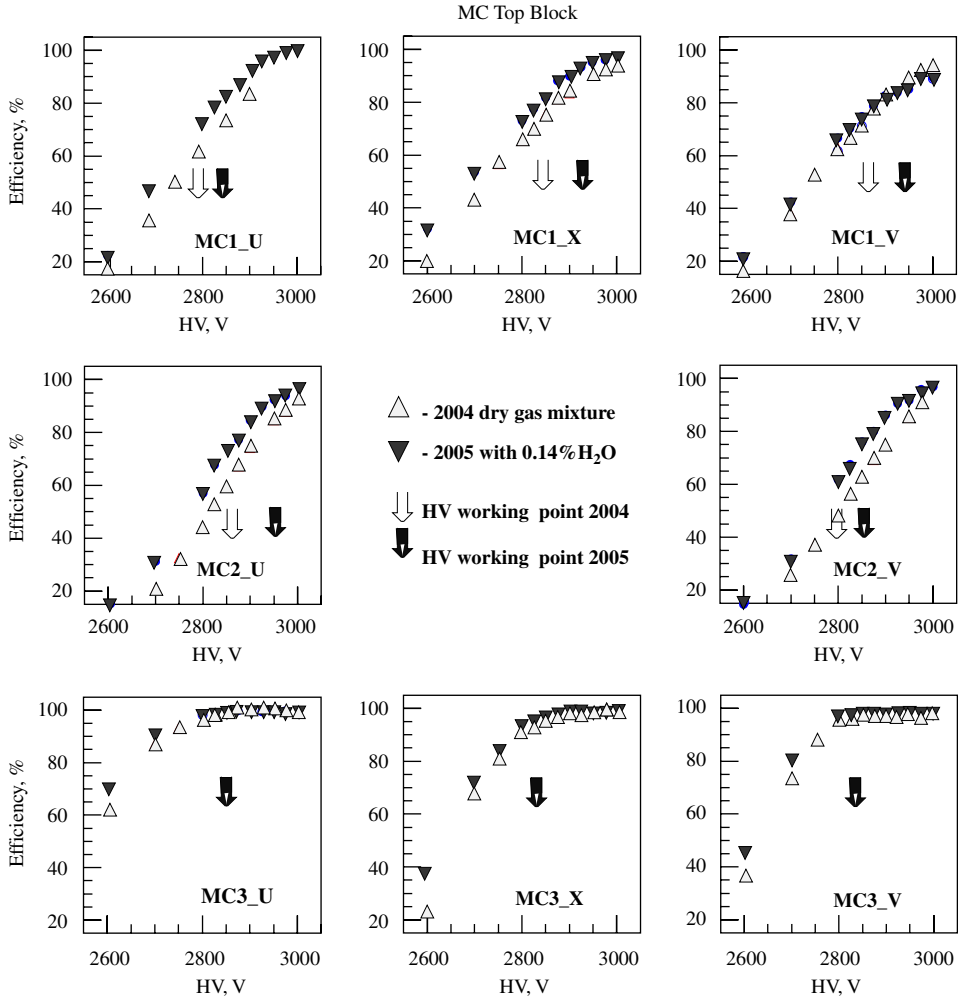

Fig. 10. Magnet chambers efficiency for the top block chamber versus high voltage at standard threshold used for data taken in the HERA positron beam. First measurement with dry gas mixture (▼) and next after adding of 0.14% H_2O (△).

detector without disassembly for cleaning. For this purpose, the anode and cathode wire surface were analysed after aging. The samples for this study were taken from the aged test proportional chambers. In order to understand the character of the deposits, we investigated some of the damaged wires using Scanning Electron Microscopy and X-ray emission (0–10 keV) spectroscopy (SEM/XEM).

5.1. Results of the SEM/XEM analysis

Observation of the disassembled aged test chamber TC1 showed a clear presence of deposits on the anode wires in the area exposed to the ^{90}Sr source. At the centre of the irradiated zone, the gold covering looked damaged and had become dark brown. However, the non-irradiated wires had no noticeable change. Fig. 11 shows the SEM micrograph of part of the irradiated anode wire, which was taken from the fifth test point (see Fig. 6). The whole wire surface is coated by the deposits. Examination of some locations with XEM showed a prominent peak of silicon and a weak presence of tungsten and oxygen. Therefore, MCs aging is associated with deposition of silicon on the anode wires.

Almost the entire cathode plane surface had temper colours circles concentrated between the irradiated zone and the gas outlet. In Fig. 12 is presented the result of SEM/XEM examination of a cathode wire taken from the irradiated zone at test point 5. Hardly any deposits can be seen in the SEM micrograph. Some white spots on the surface were identified as silicon. The presence of oxygen implies a slight oxidation of the copper surface. The traces of carbon and fluorine are definitely remnants of $CF_3^{\bullet}$ and $CF_2^{\bullet\bullet}$ radicals and positive ions produced due to electron impact dissociation of CF_4 (dissociation energy $E_{dis.} = 5.2$ eV) in an avalanche near the anode wire [6] due to mechanisms such as

$$e^- + CF_4 \rightarrow CF_3^{\bullet} + F + e^- \quad (4)$$

$$e^- + CF_4 \rightarrow CF_3^+ + F^- + e^- \quad (5)$$

$$e^- + CF_4 \rightarrow CF_3^- + F^{\bullet}. \quad (6)$$

The growth of metal fluorides on the copper wires aged in CF_4 was described by the authors of Ref. [12]. Another mechanism leading to the formation of CF_3^+ may be the dissociative charge transfer reaction:

$$Ar^+ + CF_4 \rightarrow CF_3^+ + F + Ar. \quad (7)$$

It may take place both after ^{90}Sr ionisation and in avalanche discharge. The authors in Ref. [13] estimate that at Ar^+ energies between 0.02 and 2 eV, the process operates with an efficiency close to 100%. The drift time of the CF_3^+ ions to the cathode plane of the chamber is a few milliseconds and distribution is not affected by the gas flow. Traces of fluorine were found only in vicinity of the irradiated zones.

To compare with results in the test point 5, the SEM/XEM analysis was done of a cathode wire surface taken from the non-irradiated 'Malter zone' at the sixth test point (see Fig. 13). One observes carbon, which deposited as flakes on the wire surface, and trace of the oxidated copper.

One source of the carbon and oxygen is CO_2 dissociation due to the electron impact in the avalanche ($E_{dis.} = 5.5$ eV)

$$e^- + CO_2 \rightarrow CO^{\bullet} + O^{\bullet} + e^- \quad (8)$$

$$e^- + CO_2 \rightarrow CO^{\bullet} + O^- \quad (9)$$

$$e^- + CO_2 \rightarrow CO^- + O^{\bullet} \quad (10)$$

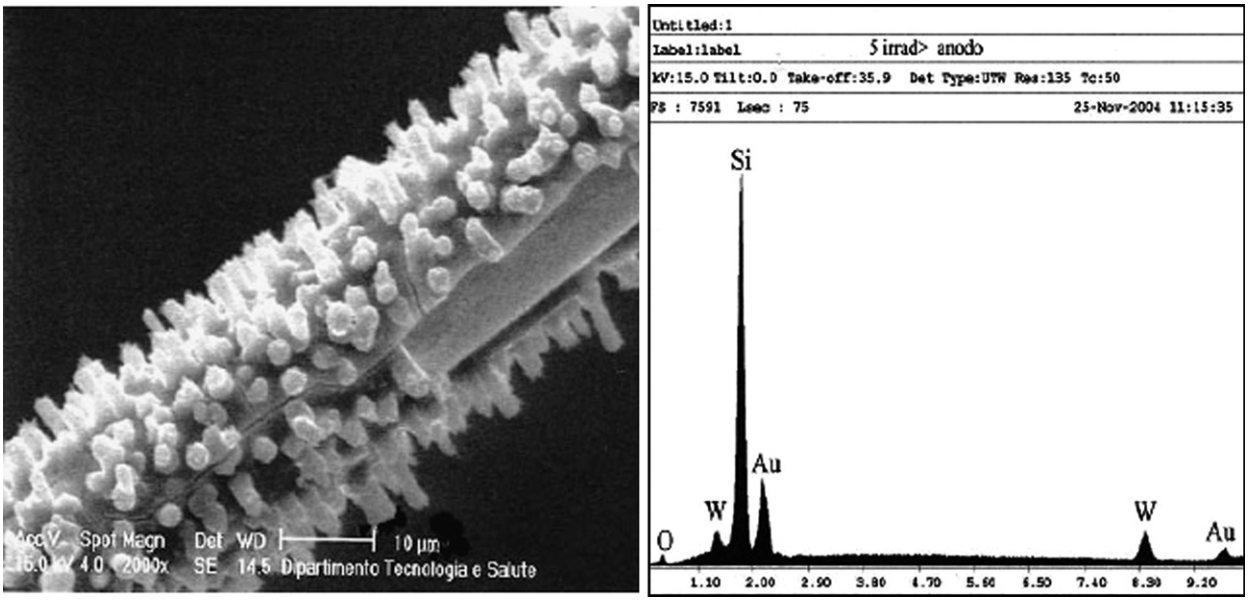

Fig. 11. SEM micrograph of the anode wire irradiated in the fifth test point (see Fig. 6) after accumulation of $Q_{anode}^{point\ 5} = 32$ mC/cm and XEM spectra of the deposits on the surface.

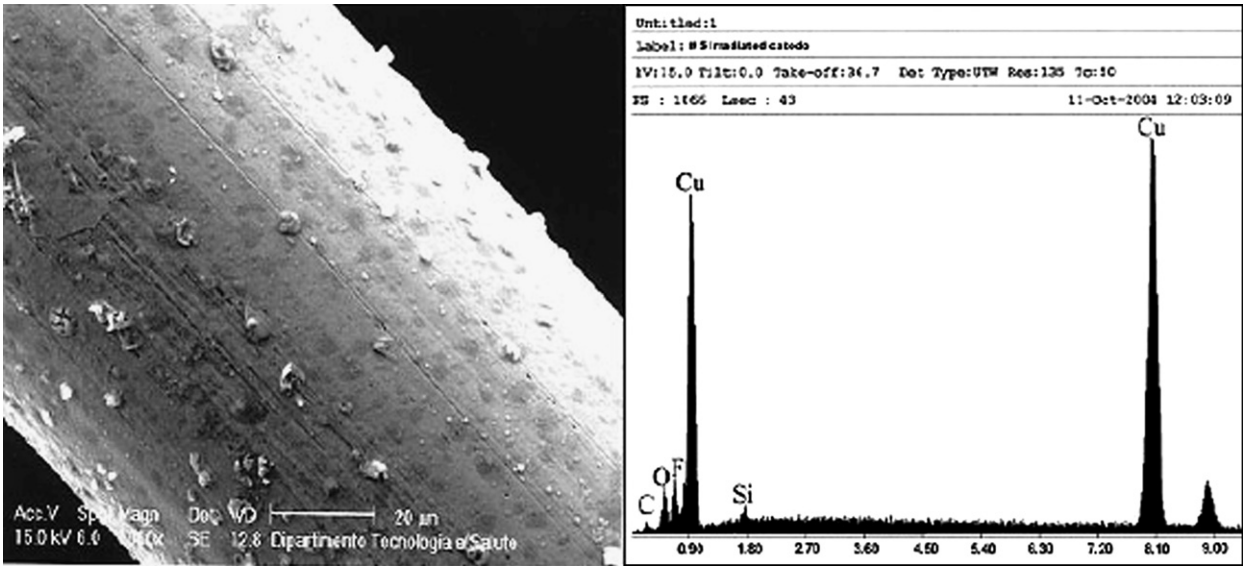

Fig. 12. SEM micrograph of the irradiated in the fifth test point (see Fig. 6) cathode wire after accumulation of $Q_{\text{cathode}} = 4.75\,\text{mC/cm}$ and XEM spectra of the deposits on the surface.

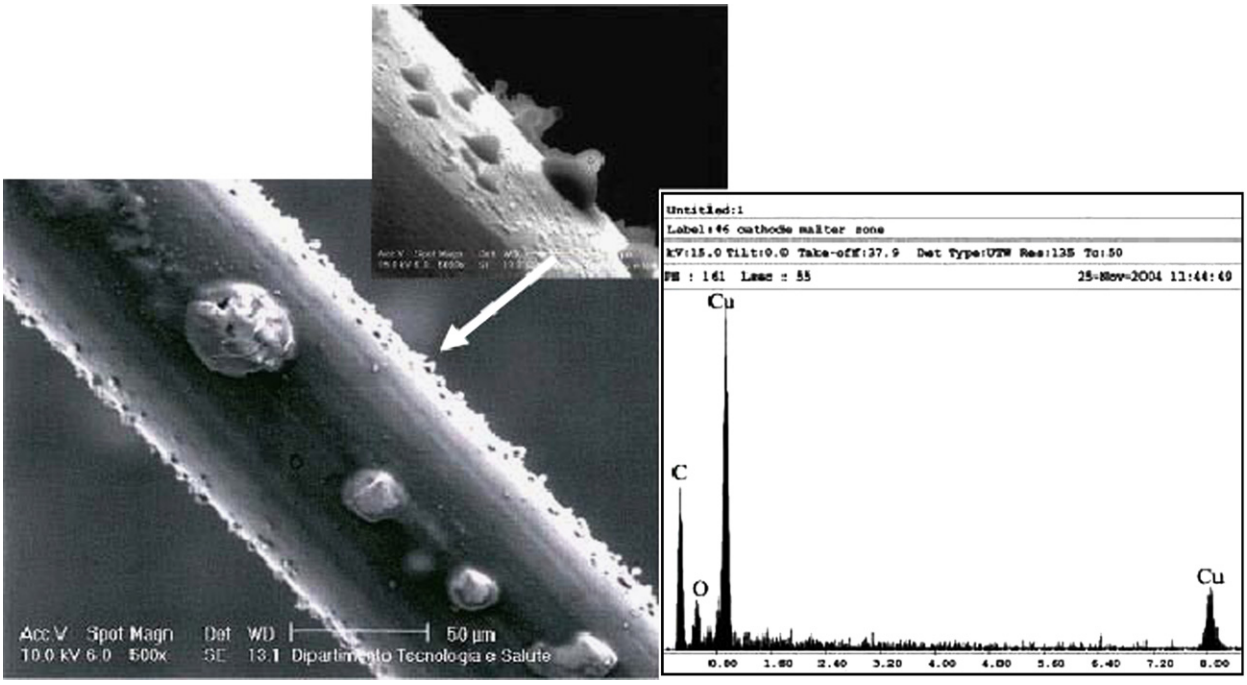

Fig. 13. SEM micrograph of the cathode wire from the non-irradiated sixth test point, see Fig. 6, after accumulated charge of $Q_{\text{cathode}} = 4.75\,\text{mC/cm}$ and XEM spectra of the deposits on the surface.

$$e^- + CO_2 \rightarrow C^{\bullet} + O^{\bullet} + e^-. \quad (11)$$

Normally, copper oxidation goes as a sequence $Cu \rightarrow Cu_2O \rightarrow Cu_2O_3 \rightarrow CuO$ resulting in a high resistive layer on the wire surface. Hence, appearance of resistive copper oxides together with carbon flakes on the cathode wires appears to be the reason for the Malter effect.

The test proportional chamber (TC2) with accumulated charge up to $Q_{\text{anode}}^{\text{point 5}} = 44\,\text{mC/cm}$ in the point 5 with hydrated gas mixture was also examined. Since this chamber exhibited stable characteristics during the test, the deposits were not expected. The visual inspection of the opened chamber confirmed this. The results obtained by the SEM/XEM analysis are presented in Fig. 14. One sees in the SEM micrograph an almost clean and undamaged gold surface of the anode wire taken from the irradiated zone. The XEM analysis shows a small peak of silicon, which is evident as white tiny nodes on the wire surface. Apparently, water prevented the silicon deposition on the wires. The SEM/XEM examination of the cathode wires

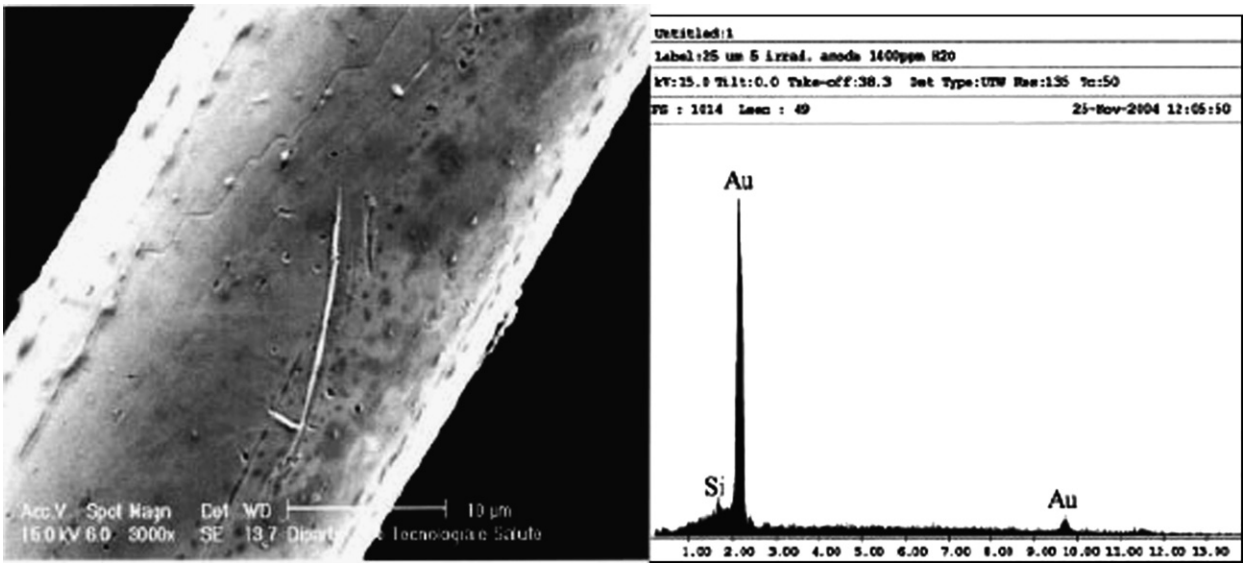

Fig. 14. SEM micrograph of the anode wire irradiated with gas mixture containing 0.14% H_2O after dose of $Q_{\text{anode}}^{\text{point 5}} = 44\,\text{mC/cm}$ and XEM spectra of the deposits on the surface.

does not show any materials besides copper with a weak peak of oxygen much smaller than the peaks shown in Figs. 12 and 13.

Thus the effectiveness of adding water to the gas mixture used in the MCs has been demonstrated at an accumulated charge of 50 mC/cm.

5.2. Recovery of the aged anode wires

In order to develop a method to non-invasively recover deteriorated gas detectors a fourth test proportional chamber (TC4) was irradiated up to the accumulated charge $Q_{\text{anode}} = 18.7\,\text{mC/cm}$ with a standard MCs gas mixture. This resulted in the gas gain degradation in the irradiated zone, which we attempted to restore.

5.2.1. Choice of gas composition

To remove the silicon coatings from the aged anode wires, we used a technique taken from the manufacturing process of semiconductor components. RF-plasmas based on CF_4 have been used for many years to remove Si and SiO_2 in integrated circuit production. Chemical reactions between the discharge-generated atoms and radicals ($F^{\bullet}, CF_3^{\bullet}, CF_2^{\bullet}$) and silicon occur at the surface at positive potential, producing SiF_4 which desorbs into gas phase and is evacuated with the gas flow.

In Ref. [14] the authors demonstrated cleaning of SiO_2-coated anode wires using a glow discharge of a 80% $CF_4 + 20\%C_4H_{10}$ gas mixture. Similarly, carbon was removed from the anode and cathode surfaces in work [15]. Aged drift tubes were operated with reversed high voltage using pure argon and a $99\%Ar + 1\%O_2$ mixture at glow discharge mode with current in the range of 0.7–23 μA/cm.

Utilising this experience to recover the aged wires, we choose a $80\%CF_4 + 20\%CO_2$ gas mixture. To simulate Si etching conditions in glow discharge, the reversed potential was applied. As noted in Refs. [16,17] the electric field accelerates positive CF_3^+ ions and causes ion bombardment of the electrode. This significantly enhances the etching of silicon in the formation of integrated circuits. Typically, the process is carried out in the pressure range of 10–200 Torr with an ion energy ranging from zero to a few hundred eV. Although the field to pressure ratio in the proportional chamber is about 400 V/cm Torr, which is about 10 times greater than that in the RF-plasma, we assumed that ions bombardment to be about the same in this case.

The CF_4 concentration 80% for Si etching was chosen from Ref. [12]. Adding CO_2 to the gas mixture enhances both the Si [18] and carbon [15] etching of the wires in the CF_4 discharge. Note that the copper of the cathode wire is etched less in our recovery procedure as it does not form a volatile fluoride. However, some copper will be removed by sputtering.

5.2.2. Result of recover procedure

Training of the aged test proportional chamber at 15–20 nA/cm glow discharge and ^{55}Fe current during 70 h demonstrated a complete recover of the aged detector.

The recovery procedures used a glow discharge operation mode with irradiation of the damaged zone by ^{55}Fe γ-rays from a 2 kHz source. The 6 keV gammas maintained by gas ionisation the glow discharge plasma and improved the etching conditions by breaking of the chemical bonds of the anode coating deposits. In Fig. 15a one can see the degradation of the gas gain, and in Fig. 15b one can see the recovery of the aged zone after $Q_{\text{anode}} \sim 1.5\,\text{mC/cm}$. Because the ^{55}Fe spectrum exhibits a sufficiently narrow peak in the CF_4/CO_2 gas mixture it was used for monitoring of the gas gain during the recovery procedure. To have a well-characterised degradation to recovery pattern, the

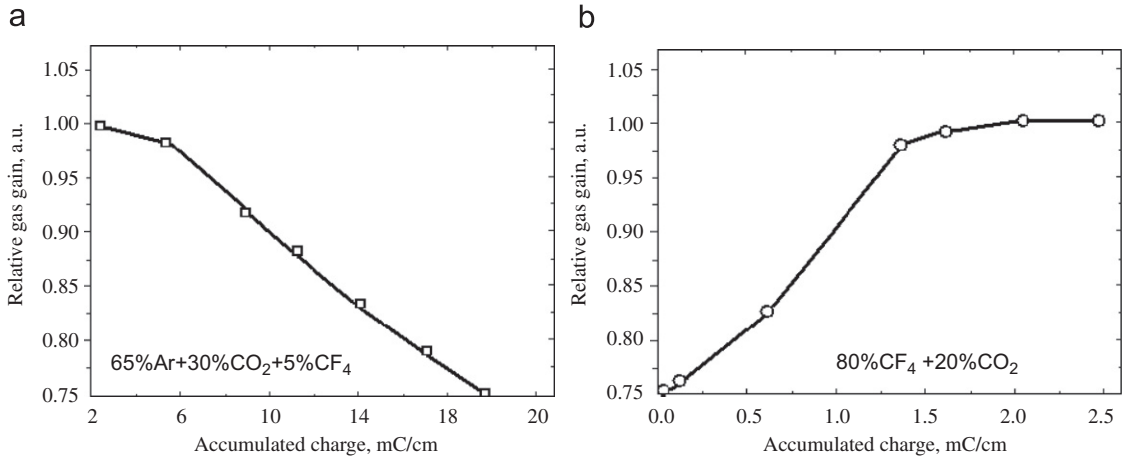

Fig. 15. (a) Dependence of the relative gas gain in the zone irradiated by ^{90}Sr versus charge accumulated by the anode wires. The aging performed using magnet chambers gas mixture. (b) Dependence of the relative gas gain during the recovery procedure with glow discharge versus the accumulated charge of the anode wires.

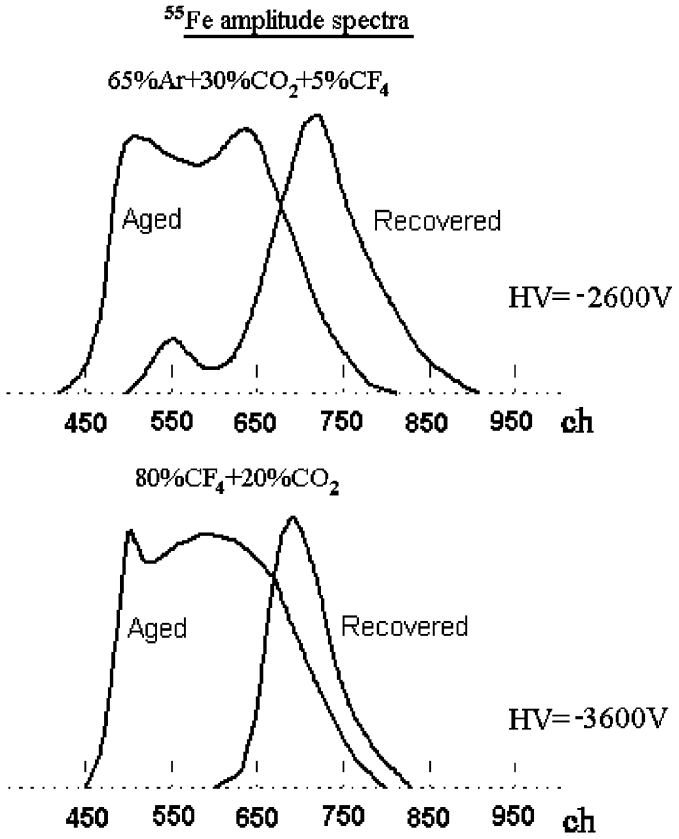

Fig. 16. A comparison of the charge spectrum shape after exposure to gas mixtures $Ar/CO_2/CF_4$ and $CF4/CO_2$.

shape of the ^{55}Fe spectrum was measured at the beginning and at the end of the training run using the MC gas mixture. In Fig. 16 is presented a comparison of the change in the charge spectrum shape using the charge spectrum shape both gas mixtures $Ar/CO_2/CF_4$ and CF_4/CO_2.

Fig. 17 shows the results of aging and recovery in terms of the count rates from the ^{55}Fe source with 3 mm diameter

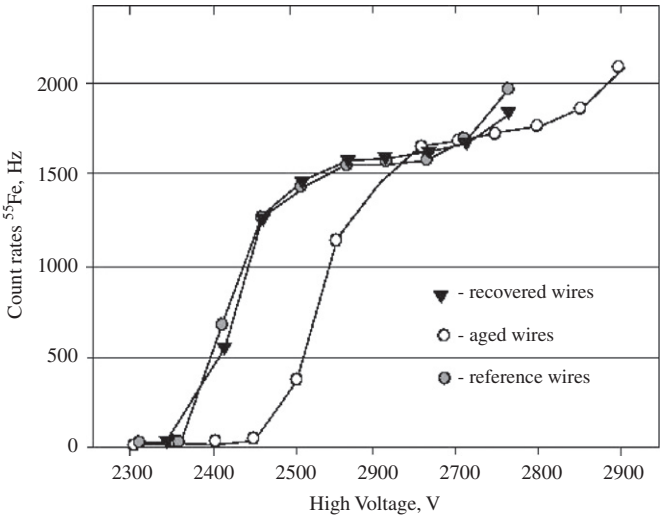

Fig. 17. Count rates from ^{55}Fe γ-ray source measured after aging and recovery procedure as a comparison with the count rate from the reference non-irradiated zone.

collimator. After recovery practically no difference is seen with reference wires.

Clearly, at maximum accumulated charge $Q_{\text{anode}} = 18.7\,\text{mC/cm}$ that corresponds only to $Q_{\text{cathode}} = 0.94$ mC/cm, we could not observe cathode aging. A follow up study of the recovering properties of the CF_4/CO_2 mixture using the aged MC modules appears attractive.

6. Summary

During installation to prepare for the HERMES experiment, it is assumed that the gas supply system to the MCs was accidentally contaminated with silicon-based oil. As a result, aging deterioration of the proportional chambers started at a small accumulated charge $Q \leqslant 10\,\text{mC/cm}$. Efficiency thereby degraded and the appearance of a Malter current was observed.

Because of the continuous operation of the experiment and inaccessibility of the proportional chambers inside the spectrometer's magnet gap, we had no opportunity to reach the damaged detector. To find a non-invasive remedy against the developing aging effect, a study with test versions of the MCs was performed. It was found that adding of 0.14% H_2O to the gas mixture 65%Ar + 30% CO_2 + 5%CF_4 alleviates the aging effect, although it does not clean the anode wires. The Malter current was cancelled and this permitted a higher voltage W.P., which compensated the efficiency degradation.

A system providing a precise addition of water to the gas mixture was designed. Using hydration of the gas mixture in the MC gas system, the aging development was stopped. For three years the MCs demonstrated a stable and reliable operation in the HERMES experiment.

A technique to complete recover the aged proportional chamber was demonstrated. A follow up study of the recovery effect on the cathode wires is needed. It looks attractive to apply the recovery method with the 80%CO_2 + 20%CF_4 gas mixture to the real aged MCs after the end of the HERMES experiment.

Acknowledgements

The authors are very grateful to Richard Conti (IBM, USA) and Rob Veenhof (CERN, Switzerland) for reading and kindly correcting this manuscript.

References

[1] Andreev, et al., Nucl. Instr. and Meth. A 465 (2001) 482.
[2] K. Ackerstaff, et al., Nucl. Instr. and Meth. A 417 (1998) 230.
[3] J.A. Kadyk, Nucl. Instr. and Meth. A 300 (1991) 436.
[4] L. Malter, Phys. Rev. 50 (1936) 48.
[5] F. Sauli, Nucl. Instr. and Meth. A 515 (2003) 1.
[6] J. Va'vra, Nucl. Instr. and Meth. A 367 (1995) 353.
[7] A.M. Boyarski, Nucl. Instr. and Meth. A 515 (2003) 190.
[8] D. Bailay, R. Hall-Wilton, Nucl. Instr. and Meth. A 515 (2003) 37.
[9] T. Ferguson, et al., Nucl. Instr. and Meth. A 488 (2002) 240.
[10] J. Buerger, et al., Nucl. Instr. and Meth. A 279 (1989) 217;
S. Masson, Ph.D. Thesis, PITHA94/50, RWTH Aachen, 1994.
[11] A. Schreiner, et al., Nucl. Instr. and Meth. A 515 (2003) 146.
[12] J. Wise, J.A. Kadyk, J. Appl. Phys. 74 (9) (1993).
[13] E. Basurto, J. de Urquijo, J. Appl. Phys. 91 (1) (2002).
[14] R. Openshaw, R.S. Henderson, et al., IEEE Trans. Nucl. Sci. NS-34 (1987) 528.
[15] M. Kollenfrath, V. Paschhoff, M. Spegel, et al., Nucl. Instr. and Meth. A 419 (1998) 451;
V. Paschhoff, Inaugural-Dissertation, Universitaet Freiburg, Facueltet fuer Physik, October 1999.
[16] G.S. Oehrlen, J.F. Rembetski, IBM J. Res. Dev. 36 (2) (1992).
[17] J.W. Coburn, Plasma Etching and Reactive Ion Etching, American Vacuum Society, New York, 1982.
[18] K.R. Ryan, I.C. Plumb, Plasma Chem. Plasma Process. 6 (3) (1986).